The Astrophysical Journal Letters, 893:L46 (5pp), 2020 April 20 https://doi.org/10.3847/2041-8213/ab881d

Dynamic Kink Instability and Transverse Motions of Solar Spicules

Teimuraz V. Zaqarashvili[1,2,3]
[1] IGAM, Institute für Physik, University of Graz, Universitätsplatz 5, A-8010 Graz, Austria; teimuraz.zaqarashvili@uni-graz.at
[2] Ilia State University, Cholokashvili ave 5/3, Tbilisi, Georgia
[3] Abastumani Astrophysical Observatory, Mount Kanobili, Abastumani, Georgia
Received 2020 March 10; revised 2020 April 4; accepted 2020 April 8; published 2020 April 24

Abstract

Hydrodynamic jets are unstable to the kink instability ($m = 1$ mode in cylindrical geometry) owing to the centripetal force, which increases the transverse displacement of the jet. When the jet moves along a magnetic field, the Lorentz force tries to decrease the displacement and stabilize the instability of sub-Alfvénic flows. The threshold of the instability depends on the Alfvén Mach number (the ratio of Alfvén and jet speeds). We suggest that the dynamic kink instability may be important to explain observed transverse motions of type II spicules in the solar atmosphere. We show that the instability may begin for spicules that rise up at the peripheries of vertically expanding magnetic flux tubes because of the decrease of the Alfvén speed in both the vertical and the radial directions. Therefore, inclined spicules may be more unstable and have higher transverse speeds. Periods and growth times of unstable modes in the conditions of type II spicules have values of 30 s and 25–100 s, respectively, which are comparable to the lifetime of the structures. This may indicate an interconnection between high-speed flow and the rapid disappearance of type II spicules in chromospheric spectral lines.

Unified Astronomy Thesaurus concepts: Solar spicules (1525); Solar chromosphere (1479); Solar mottles (1074)

1. Introduction

Spicules are dense chromospheric plasma jets flowing upward into hot and tenuous coronae (Beckers 1968). They are usually observed in chromospheric Hα, D_3, and Ca II H lines at the solar limb. The disk counterparts of spicules are mottles, which have almost the same properties as spicules (Tsiropoula & Schmieder 1997). The typical lifetime and upward velocity of classical spicules/mottles are 5–15 minutes and ~20–30 km s^{-1}, respectively. Recent Hinode/SOT observations with high spatial and temporal resolutions (De Pontieu et al. 2007a) revealed another type of spicule (type II). Rouppe van der Voort et al. (2009) reported disk counterparts of type II spicules named Rapid Blue/Rapid Red shifted excursions (RBEs/RREs). Both type II spicules and RBEs/RREs have much shorter lifetimes (about 10–150 s) and higher upward velocities (50–150 km s^{-1}) than classical (type I) spicules in Ca II H (De Pontieu et al. 2007a), Hα (Kuridze et al. 2015), and Lyα (Chintzoglou et al. 2018) lines. However, recent studies combining observations from Hinode, VAULT2.0, and the Interface Region Imaging Spectrograph (IRIS) showed that after disappearance in chromospheric lines many type II spicules appear in hotter lines like Mg II, C II, and Si IV (Pereira et al. 2014; Rouppe van der Voort et al. 2015; Skogsrud et al. 2015; Chintzoglou et al. 2018).

Observations show that spicules undergo continuous transverse motion of their axes. Type I spicules and mottles show obvious oscillatory transverse motions of axes with periods of 30–500 s interpreted as Alfvén and/or magnetohydrodynamic (MHD) kink waves (Kukhianidze et al. 2006; De Pontieu et al. 2007b; Zaqarashvili et al. 2007; Zaqarashvili & Erdélyi 2009; Okamoto & De Pontieu 2011; Kuridze et al. 2012; Tsiropoula et al. 2012). On the other hand, the short lifetime of type II spicules and RBEs/RREs in chromospheric lines complicates the observation of the full swing of the axes, but most of the structures show a linear trend of transverse motion (Kuridze et al. 2015): the structures move in a transverse direction and do not return back, but rather they disappear. Moreover, the transverse velocity is about 8 km s^{-1} in mottles (Kuridze et al. 2012) and almost twice (14–17 km s^{-1}) in RBEs/RREs (Kuridze et al. 2015). Do type II spicules disappear over a shorter time period than the oscillation period? No existing mechanism supports such strong damping of oscillations and corresponding heating. Even if such strongly damped oscillations exist, then why they are not damped in type I spicules? On the other hand, the appearance of spicules in IRIS spectral lines show that type II spicules are rapidly heated to transition region (TR) temperatures (Pereira et al. 2014), though the heating mechanism is not yet completely clear. Ion–neutral collisions, Kelvin–Helmholtz instability, or both together might lead to the rapid heating (Kuridze et al. 2016; Martínez-Sykora et al. 2017; Antolin et al. 2018), but it is not yet fully established. If spicules are rapidly heated, then their axes may continue to oscillate in TR lines. Another possibility is that the spicules are quickly destroyed by some instability process. This point is still open for further discussion.

De Pontieu et al. (2012) showed that type II spicules are characterized by the simultaneous action of three different types of motion such as field-aligned flows, or swaying and torsional motions, though the field-aligned flows are few times stronger than the others. In this Letter, we assume that spicules are field-aligned jets and propose that the dynamic kink instability of jets could explain the observed transverse (swaying) motion of spicule axes. The dynamic instability of jets is well known in nonmagnetic fluid dynamics, where the jets show antisymmetric displacement of axis (Drazin 2002). In cylindrical geometry, axially symmetric nonmagnetic jets have the vorticity component in the ϕ direction, hence they can be considered as vortically twisted tubes. Therefore, the jets are unstable to the dynamic kink instability very similar to the magnetically twisted tubes, which are unstable to the MHD kink instability. Flow-aligned magnetic field usually stabilizes sub-Alfvénic jets, but super-Alfvénic jets still can be unstable to the dynamic kink instability. This process can be of importance in high-speed type II spicules and RBEs/RREs.

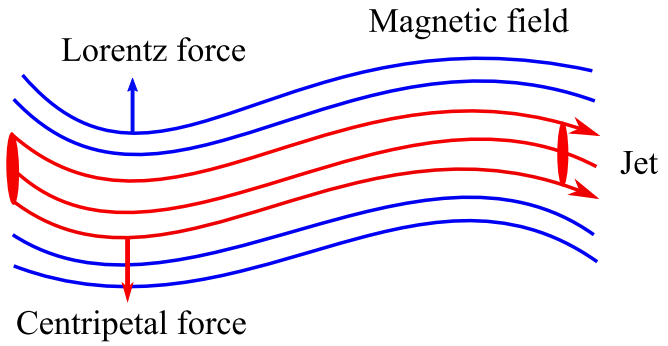

Figure 1. Dynamic kink instability of jets (red lines) in the magnetic field (blue lines). Red (blue) arrow show the direction of the centripetal force of flow (Lorentz force). The centripetal force tries to amplify the transverse displacement, while the Lorentz force tries to reduce it. When the centripetal force is stronger, then the displacement is unstable.

2. Dynamic Kink Instability in Jets

We consider a homogeneous cylindrical jet of uniform velocity U_z, radius a and density ρ_0, which moves in a medium of uniform density, ρ_e, along an uniform magnetic field, B_z. This is a very simplified case compared to the complex structure of the solar chromosphere, though the consideration shows basic properties of the instability. The linear incompressible dynamics of the jet is governed by the dispersion equation (see details in the Appendix)

$$(\rho_e E_m - \rho_0)\omega^2 + 2\rho_0 k_z U_z \omega - (\rho_0 k_z^2 U_z^2 + \rho_e k_z^2 V_{\rm Ae}^2 E_m - \rho_0 k_z^2 V_{\rm A0}^2) = 0, \quad (1)$$

where ω is the wave frequency, $V_{\rm Ae} = B_z/\sqrt{4\pi\rho_e}$ and $V_{\rm A0} = B_z/\sqrt{4\pi\rho_0}$ are Alfvén speeds outside and inside the jet, while $E_m(k_z a) = (I_m'(k_z a)/I_m(k_z a))(K_m(k_z a)/K_m'(k_z a))$. $I_m(k_z a)$ and $I_m(k_z a)$ are modified Bessel functions with an order m and prime sign $'$ means the differentiation with Bessel function argument. This equation can be derived from the dispersion relation of moving twisted magnetic flux tubes (Equation (25) in Zaqarashvili et al. 2014) assuming zero twist. Solution of this equation is

$$\omega = \frac{-\rho_0 k_z U_z \pm \sqrt{\rho_0\rho_e k_z^2 U_z^2 E_m + (\rho_e E_m - \rho_0)(E_m - 1)(k_z^2 B_z^2/4\pi)}}{\rho_e E_m - \rho_0}. \quad (2)$$

Here the complex frequency means the instability of the corresponding mode, where the imaginary part of frequency shows the growth rate. In the case of hydrodynamic jet (with $B_z = 0$), the antisymmetric ($m = 1$) mode always has imaginary part as $E_1(k_z a) < 0$. For long-wavelength approximation, $k_z a \ll 1$, we have $E_1(k_z a) \approx -1$ and the growth rate is $\omega_i = k_z U_z/2$ for $\rho_e = \rho_0 = \rho$. This mode leads to the transverse displacement of the jet axis (see Figure 1) and is called a kink mode (for a rectangular jet, see Drazin 2002). The similar antisymmetric mode in magnetic tubes is the MHD kink mode (Edwin & Roberts 1983). However, in static MHD, this mode is stable in non-twisted and weakly twisted tubes, but becomes unstable when the twist exceeds some critical value (Lundquist 1951), hence the mechanism for instability is the Lorentz force. In hydrodynamic jets, the kink mode is unstable

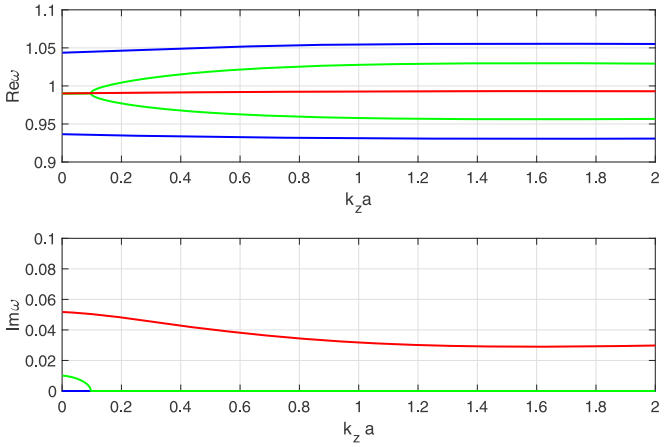

Figure 2. Real and imaginary parts of frequency vs. longitudinal wavenumber, $k_z a$. Blue, green, and red lines correspond to $V_{\rm Ae}/U_z = 0.8$, 0.7, and 0.6, respectively. Here $\rho_0/\rho_e = 100$ and the frequency is normalized by $k_z U_z$.

for any speed and wavelength. The mechanism of instability is connected to the centripetal force, which acts on the jet moving on the curved trajectory and increases the curvature (Figure 1). Therefore, the instability can be called a *dynamic kink instability* as opposed to an MHD kink instability. The jet-aligned magnetic field stabilizes the instability, as the Lorentz force is a restoring force in this case and tries to decrease the curvature (Figure 1). This is easily seen in Equation (2). If we consider the long-wavelength limit, then the second term in the square root is $4\rho k_z^2 B_z^2/4\pi$. Consequently, the frequency is real when $V_{\rm A}/U_z > 1/2$, where $V_{\rm A} = B_z/\sqrt{4\pi\rho}$ is the Alfvén speed, therefore the jet is stable. Hence, super-Alfvénic jets could be unstable to the kink instability even in non-twisted magnetic configurations. Figure 2 shows the real and imaginary parts of frequency versus longitudinal wavenumber of kink ($m = 1$) mode in dense jets (resembling spicules) for different Alfvén Mach numbers, i.e., the ratios of Alfvén and flow speeds, $V_{\rm Ae}/U_z$. The figure shows that the jet is unstable for all wavelength perturbations when the Alfvén Mach number equals 0.6 (red line). When $V_{\rm Ae}/U_z = 0.7$, then only long-wavelength perturbations ($k_z a < 0.1$) are unstable (green line). The jet is completely stable when $V_{\rm Ae}/U_z = 0.8$ (blue line). Hence, the dense jet is unstable to the dynamic kink instability when the jet speed is higher than

$$U_z > 1.25\, V_{\rm Ae}. \quad (3)$$

In the next section we study the instability in typical spicule parameters, keeping in mind that the consideration is highly simplified compared to the real structure of the solar atmosphere.

3. Dynamic Kink Instability in Spicules

Spicules are chromospheric jets rising upward into the corona, therefore they are much denser (almost two orders of magnitude) than the surrounding coronal plasma. Let us

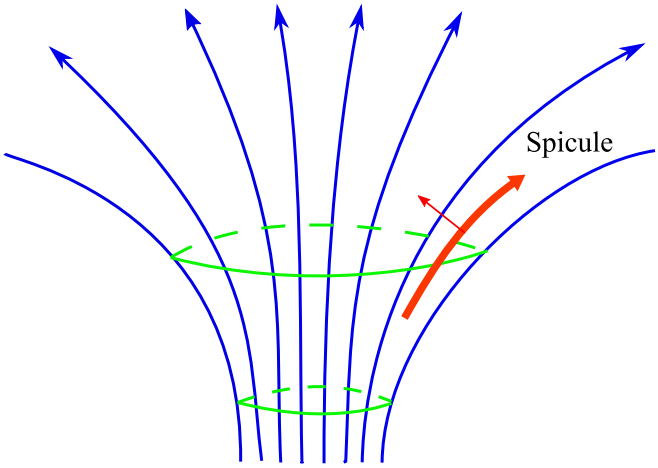

Figure 3. Sketch of an expanding magnetic flux tube. The lower green circle corresponds to the upper boundary of the chromosphere, while the upper circle may correspond to the height of $z = H_B/2$. The jet resembling a spicule (thick red arrow) moves along magnetic field lines with an angle to the vertical. The thin red arrow shows the direction of centripetal force when the jet moves along a curved trajectory.

suppose that the spicules move along magnetic field lines of expanding flux tubes, which have a much larger radius than the spicule itself (Figure 3). The magnetic field strength decreases in height as well as in the radial direction. Consequently, a spicule moving along the field line away from the tube center will "feel" a more decreased field strength than a spicule that moves along the field line at the tube center. The field components in current-free axisymmetric expanding magnetic flux tubes are

$$B_r = B_0 J_1(r/H_B) e^{-z/H_B},$$
$$B_z = B_0 J_0(r/H_B) e^{-z/H_B}, \quad (4)$$

where H_B is a scale height of the magnetic field. The Alfvén speed in the TR, say at $z = 0$, can be assumed to be 150 km s^{-1} at the tube center, $r = 0$. The pressure scale height for the TR temperature of 0.1 MK is around 5 Mm, which gives $H_B = 10$ Mm.

We first consider a spicule, which starts to flow along the field line at the tube center, $r = 0$. At the height of $z = H_B/2 = 5$ Mm, the magnetic field will drop by $\exp(1/2) = 1.65$ and the Alfvén speed will become 90 km s^{-1} (a density decrease with height will be much less influential). Then the critical flow speed will be $90 \cdot 1.25 \approx 115$ km s^{-1} (using Equation (3)) and the jet moving along the tube center with the speed of 100 km s^{-1} will by completely stable up to a height of at least 5 Mm.

We now consider a spicule that starts to flow along the field line at the distance of $r = H_B/2$ from the tube center, near $z = 0$. The magnetic field strength, $\sqrt{B_r^2 + B_z^2}$, will be decreased in height as well as in the radial direction. At $z = 0$, the field strength is decreased by 0.97 at the distance of $r = H_B/2$. In the simple case considered here, the plasma density decreases upward owing to the stratification, while it stays almost constant in the horizontal direction. Therefore, the Alfvén speed will remain unchanged at 145 km s^{-1}. As the spicule follows the same magnetic field line, it will then appear at a distance of $r \approx 1.4\, H_B$ at a height of 5 Mm. The Alfvén speed will be around 70 km s^{-1} there, which means the critical flow speed of $70 \cdot 1.25 \approx 90$ km s^{-1}; the spicule moving with 100 km s^{-1} will become unstable at this height.

Using Equation (4) one finds that the angle of the magnetic field line with regard to the vertical at $z = 0$ and $r = H_B/2$ is around 15° degree. As spicules generally follow the magnetic field lines, the angle of spicule axis with regard to the vertical will be also 15° at this position. Any spicule with the same initial speed (in our case 100 km s^{-1}), which are inclined by more than 15°, may become super-Alfvénic with height and hence become unstable. The spicules with a slower speed will require more initial inclination angle in order to become unstable with height. It is of remarkable importance that the observed median inclination angle of spicules from the vertical is 20°–40° (Beckers 1968; Tsiropoula et al. 2012). To our knowledge, there is no statistical study of inclination angle for type II spicules.

One can estimate the periods and growth times of the unstable harmonics in the conditions of spicules. Typical diameters of type I and II spicules can be assumed as 400 km and 100 km, respectively, while the typical flow speeds are 30 km s^{-1} and 100 km s^{-1}, respectively. The type I spicules are sub-Alfvénic and hence stable, while type II spicules are close to the Alfvén speed, and some may be in the instability region. The dependence of periods and growth times of the unstable harmonics with $k_z a = 0.1$ on the Alfvén Mach number is shown in Figure 4. The period of unstable harmonics in type II spicules is almost independent of flow parameters and is around 31–32 s, while the growth time crucially depends on the Alfvén Mach number and the density ratio. For the Mach number of $V_{Ae}/U_z = 0.6$, the growth time is 100 s for $\rho_0/\rho_e = 100$ and 45 s for $\rho_0/\rho_e = 25$. Hence, type II spicules are strongly unstable to the dynamic kink instability and the growth time has the same order as the period. It is interesting that the growth time is of the same order as the observed lifetime of type II spicules in Ca II H line; therefore, one can suggest a connection between the instability and observed transverse motion of the structures. One can assume that the axes of type II spicules start rapid transverse motions owing to the instability and make a back-and-forth swing when the growth time is longer than the period i.e., for $1.25\, V_{Ae} < U_z < 2\, V_{Ae}$. On the other hand, the spicule may show only linear transverse motion without full swing when the growth time is shorter than the period i.e., for $U_z > 2\, V_{Ae}$. This means that the very high-speed spicules may be destroyed because of instability before they return back to their initial position.

4. Discussion and Conclusion

Observed transverse displacement of spicule axis has been suggested to be caused either by volume-feeling Alfvén waves or MHD kink waves (Kukhianidze et al. 2006; De Pontieu et al. 2007b; Zaqarashvili & Erdélyi 2009; Okamoto & De Pontieu 2011). In both cases, the transverse motion is the result of the Lorentz force acting on magnetic field lines. Here, we suggest an alternative mechanism for the transverse displacement. The mechanism is connected to the centripetal force of jet flowing along the curved trajectory: when the axis of hydrodynamic jet is deformed, then the force tries to amplify the displacement and leads to the kink instability as shown on Figure 1. If the jet flows along the magnetic field, then the Lorentz force tries to straighten the field lines and hence acting against instability. The ratio of Alfvén to the jet speeds defines the critical threshold for the dynamic kink instability. For dense jets in

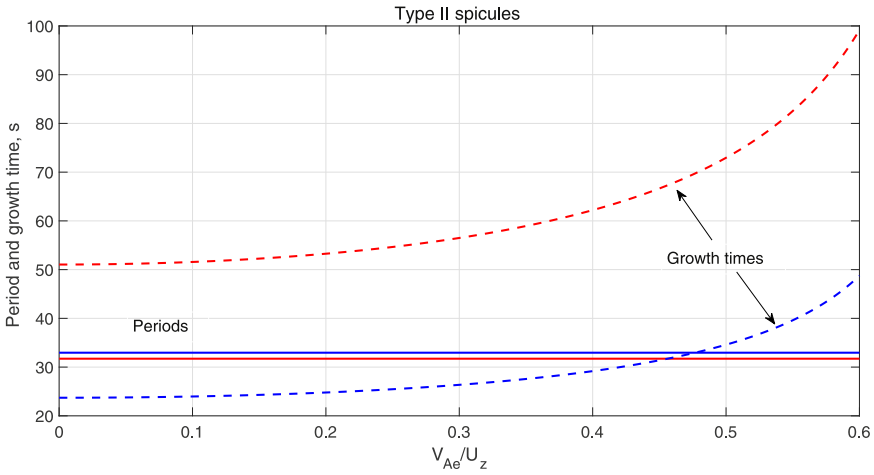

Figure 4. Periods (solid lines) and growth times (dashed lines) of unstable modes with $k_z a = 0.1$ vs. Alfvén Mach number $V_{\rm Ae}/U_z$. The flow speed and diameter of type II spicules are assumed to be $U_z = 100$ km s^{-1} and $2a = 100$ km, respectively. Blue and red colors correspond to the density difference of $\rho_0/\rho_e = 25$ and $\rho_0/\rho_e = 100$, respectively.

rarified environments (resembling spicules), the instability may start for $U_z > 1.25\, V_{\rm Ae}$. The velocity of type I spicules is less than Alfvén speed in the lower corona. However, the speed of type II spicules is comparable (perhaps under certain circumstances) to the external Alfvén speed, which may lead to the dynamic kink instability in these structures.

Spicules probably follow the magnetic field lines when they rise up into the corona. The magnetic field obviously changes its structure from the chromosphere to the corona expanding upward, which suggests that the Alfvén speed should be also inhomogeneous in vertical and horizontal directions. Therefore, the conditions for the dynamic kink instability for type II spicules may arise only in certain regions where the flow becomes super-Alfvénic. This may happen in peripheries of expanding magnetic flux tubes (Figure 3), where the negative gradient of the Alfvén speed has maximal value owing to the volume expansion of magnetic field lines and the minimization of the density stratification effect (Hollweg et al. 1982; Grant et al. 2018). Spicules flowing along the field lines at the central axis of an expanding magnetic flux tube may stay sub-Alfvénic, and hence stable to the dynamic kink instability. On the other hand, spicules starting to flow along the field lines away from the tube axis (as on Figure 4) may become super-Alfvénic owing to the negative gradient of Alfvén speed, and hence become unstable. In the case of a simple expanding magnetic flux tube with the Alfvén speed of 150 km s^{-1} at $z = 0$, the jet with 100 km s^{-1} speed become unstable to the dynamic kink instability at a height of 5 Mm if it starts to flow along the field line at the distance $r = H_B/2$ from the tube center. This field line has an inclination angle of 15°, therefore the spicule will be also inclined with the same angle to the vertical. All spicules that started with $>15°$ angle at $z = 0$ (corresponding to the upper boundary of the chromosphere) and with a speed of 100 km s^{-1} can become unstable when they move upward, assuming the physical properties and constraints assumed here. More inclined spicules must show a stronger transverse velocity. It may also happen that less-inclined spicules may show a full swinging transverse motion, while the more inclined ones only a linear transverse trend. It would be interesting to check the dependence of transverse velocity and dynamics on the inclination angle of type II spicules observationally.

The rapid disappearance of type II spicules in chromospheric spectral lines might be also connected to the dynamic kink instability, as it may lead to the destruction of the structure. However, most of the spicules appear in hotter TR lines (Pereira et al. 2014; Rouppe van der Voort et al. 2015; Skogsrud et al. 2015; Chintzoglou et al. 2018), which probably indicates rapid heating during transverse motion rather than decomposition. The heating mechanism might be ion–neutral collisions (Erdélyi & James 2004; Martínez-Sykora et al. 2017), Kelvin–Helmholtz instability (Antolin et al. 2018), or both effects simultaneously (Kuridze et al. 2016).

Periods and growth times of unstable modes are estimated to be ∼30 s and 25–100 s, respectively, in the conditions of type II spicules. On the other hand, type I spicules seem to be generally stable to the kink instability. It is interesting to note that the period and growth times of unstable harmonics in type II spicules are comparable to the range of their lifetimes in chromospheric lines. This may indicate a link between dynamic kink instability and the evolution of these structures. The suggested scenario is simple: the type II spicules moving upward with an angle to the vertical (for example, near the peripheries of expanding magnetic flux tubes) may become super-Alfvénic at certain heights owing to the negative gradient of Alfvén speed, and hence unstable to the dynamic kink instability. Then the axis of the spicules may start transverse motions, which might lead either to the complete destruction of the spicule because of instability or the rapid heating by some mechanism up to the TR temperature. In the first case, spicules will rapidly disappear in all spectral lines. In the second case, spicules will disappear in chromospheric spectral lines, but appear in hotter TR lines, as has been found by observations. The inclination angle of type II spicules might play a significant role in both processes, which can be tested by observations.

It must be noted that the consideration in this Letter is rather simple, capturing only the basic properties of instability and not taking into account observed velocity/density gradients (Sekse et al. 2012) or torsional motions (De Pontieu et al. 2012). Therefore, more analytical/numerical and observational study is necessary.

The work was funded by the Austrian Science Fund (FWF, project P30695-N27).

Appendix
Derivation of Dispersion Equation Governing a Homogeneous Jet in a Magnetic Field

We consider a homogeneous medium with uniform density, ρ_e, and homogeneous magnetic field, B_z, directed along the z-axis of cylindrical system (r, ϕ, z). A homogeneous cylindrical jet with radius a and density ρ_0 moves along the magnetic field with the uniform velocity U_z. Using Fourier analysis with $\exp(im\phi + ik_z z - i\omega t)$, where ω is the wave frequency and m, k_z are wavenumbers, one can readily find that the incompressible linear dynamics of perturbations is governed by the modified Bessel equation

$$\frac{d^2 p_t}{dr^2} + \frac{1}{r}\frac{dp_t}{dr} - \left(\frac{m^2}{r^2} + k_z^2\right)p_t = 0, \tag{A1}$$

where $p_t = p + B_z b_z/4\pi$ in total (thermal + magnetic) pressure perturbation. Solutions for the total pressure inside ($r < a$) and outside ($r > a$) the jet are $p_{ti} = a_i I_m(k_z r)$ and $p_{te} = a_e K_m(k_z r)$, respectively, where I_m and K_m are the modified Bessel functions of order m, and a_i, a_e are constants (note that the solution outside the jet is bounded at infinity). Then the Lagrangian radial displacement is governed by the expressions

$$\xi_{ri} = \frac{a_i}{\rho_0}\frac{k_z I_m^{'}(k_z r)}{(\omega - k_z U_z)^2 - k_z^2 V_{A0}^2},$$
$$\xi_{re} = \frac{a_e}{\rho_e}\frac{k_z K_m^{'}(k_z r)}{\omega^2 - k_z^2 V_{Ae}^2}, \tag{A2}$$

where $V_{Ae} = B_z/\sqrt{4\pi\rho_e}$ and $V_{A0} = B_z/\sqrt{4\pi\rho_0}$ are Alfvén speeds outside and inside the jet, while prime sign $'$ means the differentiation with Bessel function argument. Standard conditions of continuity of total pressure and displacement at the jet boundary ($p_{ti}(a) = p_{te}(a)$, $\xi_{ri}(a) = \xi_{re}(a)$) produces the dispersion equation

$$\frac{\rho_e K_m(k_z a) I_m^{'}(k_z a)}{(\omega - k_z U_z)^2 - k_z^2 V_{A0}^2} = \frac{\rho_0 I_m(k_z a) K_m^{'}(k_z a)}{\omega^2 - k_z^2 V_{Ae}^2}. \tag{A3}$$

From this equation one can readily obtain Equation (1) of the main text

$$(\rho_e E_m - \rho_0)\omega^2 + 2\rho_0 k_z U_z \omega - (\rho_0 k_z^2 U_z^2 + \rho_e k_z^2 V_{Ae}^2 E_m - \rho_0 k_z^2 V_{A0}^2) = 0, \tag{A4}$$

where $E_m(k_z a) = (I_m'(k_z a)/I_m(k_z a))(K_m(k_z a)/K_m'(k_z a))$.

ORCID iDs

Teimuraz V. Zaqarashvili https://orcid.org/0000-0001-5015-5762

References

Antolin, P., Schmit, D., Pereira, T. M. D., De Pontieu, B., & De Moortel, I. 2018, ApJ, 856, 44
Beckers, J. M. 1968, SoPh, 3, 367
Chintzoglou, G., De Pontieu, B., Martínez-Sykora, J., et al. 2018, ApJ, 857, 73
De Pontieu, B., Carlsson, M., Rouppe van der Voort, L. H. M., et al. 2012, ApJL, 752, L12
De Pontieu, B., McIntosh, S., Hansteen, V. H., et al. 2007a, PASJ, 59, S655
De Pontieu, B., McIntosh, S. W., Carlsson, M., et al. 2007b, Sci, 318, 1574
Drazin, P. G. 2002, Introduction to Hydrodynamic Stability (Cambridge: Cambridge Univ. Press)
Edwin, P. M., & Roberts, B. 1983, SoPh, 88, 179
Erdélyi, R., & James, S. P. 2004, A&A, 427, 1055
Grant, S. D. T., Jess, D. B., Zaqarashvili, T. V., et al. 2018, NatPh, 14, 480
Hollweg, J. V., Jackson, S., & Galloway, D. 1982, SoPh, 75, 35
Kukhianidze, V., Zaqarashvili, T. V., & Khutsishvili, E. 2006, A&A, 449, L35
Kuridze, D., Henriques, V., Mathioudakis, M., et al. 2015, ApJ, 802, 26
Kuridze, D., Morton, R. J., Erdélyi, R., et al. 2012, ApJ, 750, 51
Kuridze, D., Zaqarashvili, T. V., Henriques, V., et al. 2016, ApJ, 830, 133
Lundquist, S. 1951, PhRv, 83, 307
Martínez-Sykora, J., De Pontieu, B., Hansteen, V. H., et al. 2017, Sci, 356, 1269
Okamoto, T. J., & De Pontieu, B. 2011, ApJL, 736, L24
Pereira, T. M. D., De Pontieu, B., Carlsson, M., et al. 2014, ApJL, 792, L15
Rouppe van der Voort, L., De Pontieu, B., Pereira, T. M. D., Carlsson, M., & Hansteen, V. 2015, ApJL, 799, L3
Rouppe van der Voort, L., Leenaarts, J., de Pontieu, B., Carlsson, M., & Vissers, G. 2009, ApJ, 705, 272
Sekse, D. H., Rouppe van der Voort, L., & De Pontieu, B. 2012, ApJ, 752, 108
Skogsrud, H., Rouppe van der Voort, L., De Pontieu, B., & Pereira, T. M. D. 2015, ApJ, 806, 170
Tsiropoula, G., & Schmieder, B. 1997, A&A, 324, 1183
Tsiropoula, G., Tziotziou, K., Kontogiannis, I., et al. 2012, SSRv, 169, 181
Zaqarashvili, T. V., & Erdélyi, R. 2009, SSRv, 149, 355
Zaqarashvili, T. V., Khutsishvili, E., Kukhianidze, V., & Ramishvili, G. 2007, A&A, 474, 627
Zaqarashvili, T. V., Vörös, Z., & Zhelyazkov, I. 2014, A&A, 561, A62